Liquid−Liquid Equilibria in Binary Mixtures Containing Substituted Benzenes with Ionic Liquid 1-Ethyl-3-methylimidazolium Bis(trifluoromethylsulfonyl)imide

Mark B. Shiflett* and Anne Marie S. Niehaus

DuPont Central Research and Development, Experimental Station, Wilmington, Delaware 19880-0304

Liquid−liquid equilibria in binary mixtures of substituted benzenes (toluene, ethylbenzene, propylbenzene, xylene isomers, trimethylbenzene isomers, aniline, nitrobenzene, phenol, and benzaldehyde) with ionic liquid, 1-ethyl-3-methylimidazolium bis(trifluoromethylsulfonyl)imide ([emim][Tf_2N]), have been measured using a mass–volume technique over a temperature range from about (293 to 373) K. Trends in both the polarity and molecular size of the solute with the immiscibility gap were discovered for the alkyl-substituted benzenes. In general, as the polarity increased and the molecular size decreased, the immiscibility gap became smaller. The nonalkyl-substituted benzenes containing functional groups (−NH_2, −NO_2, −OH, and −CHO) were completely soluble in [emim][Tf_2N] over the composition and temperature range studied. The excess molar volumes for the ionic liquid-rich side solutions range from (−1 to −5) $cm^3 \cdot mol^{-1}$, and the magnitudes are somewhat larger than those of ordinary liquid solutions. Observed LLE are well correlated by use of the nonrandom two liquid (NRTL) solution model.

Introduction

Liquid−liquid equilibria (LLE) of substituted benzenes in room-temperature ionic liquids (RTILs) are extremely important in evaluating RTILs as new solvents for chemical separation and extraction applications.[1−4] This report is a continuation of our previous studies on the phase behavior of halogenated benzene isomers in RTIL, 1-ethyl-3-methylimidazolium bis(trifluoromethylsulfonyl)imide ([emim][Tf_2N]).[5−7] The present work includes the phase behavior of toluene, ethylbenzene, propylbenzene, (*ortho*, *meta*, *para*)-xylene, (1,2,3; 1,2,4; 1,3,5)-trimethylbenzene, aniline, nitrobenzene, phenol, and benzaldehyde in [emim][Tf_2N] over a temperature range from about (293 to 373) K. We have previously studied the thermodynamic properties of RTILs with a variety of halogenated hydrocarbons,[8−17] fluorinated ethers,[18,19] and carbon dioxide.[20−25] The present phase equilibrium study of substituted benzene isomers with [emim][Tf_2N] is part of our continuing investigations to understand the interactions (or phase behaviors) of benzene compounds with RTILs.

There are several solubility studies of RTIL mixtures with aromatic hydrocarbons and alkanes in the literature;[26−34] however, to the best of our knowledge, we are the first to report LLE for many of these substituted benzene isomers in [emim][Tf_2N]. This report combines both our current work on the interactions of substituted benzenes and comparisons to our original measurements of benzene (C_6H_6) in [emim][Tf_2N].[6]

Experimental Section

Materials. Toluene (methylbenzene, C_7H_8, assay ≥ 99.9 %, Catalog and Lot no. 650579-1 L 10180EE, CAS registry no. 108-88-3), *ortho*-xylene (1,2-dimethylbenzene, C_8H_{10}, assay 98 %, Catalog and Lot no. 29,588-4 HS00958TQ, CAS registry no. 95-47-6), *meta*-xylene (1,3-dimethylbenzene, C_8H_{10}, assay ≥ 99 %, Catalog and Lot no. 29,632-5 JR21779JR, CAS registry no. 108-38-3), *para*-xylene (1,4-dimethylbenzene, C_8H_{10}, assay ≥ 99 %, Catalog and Lot no. 31,719-5 TR02257PR, CAS registry no. 106-42-3), ethylbenzene (C_8H_{10}, assay 99.8 %, Catalog and Batch no. 296848-100 ML 00749DJ, CAS registry no. 100-41-4), benzaldehyde (benzenecarbaldehyde, C_7H_6O, assay ≥ 99.5 %, Catalog and Batch no. 418099-100 ML 00196HJ, CAS registry no. 100-52-7), and aniline (phenylamine or aminobenzene, C_6H_7N, assay ≥ 99.5 %, Catalog and Batch no. 242284-100G 00914PH, CAS registry no. 62-53-3) were obtained from Sigma-Aldrich, Inc. (St. Louis, MO). Propylbenzene (C_9H_{12}, assay ≥ 99.8 %, Lot and filling code 1355771 10308207, CAS registry no. 103-65-1), 1,2,4-trimethylbenzene (pseudocumene, C_9H_{12}, assay ≥ 99.5 %, Lot and filling code 1348731 41408284, CAS registry no. 95-63-6), 1,3,5-trimethylbenzene (mesitylene or mesitelene, C_9H_{12}, assay ≥ 99.0 %, Lot and filling code 1386521 12508370, CAS registry no. 108-67-8), nitrobenzene ($C_6H_5NO_2$, assay ≥ 99.5 %, Lot and filling code 1384909 43908199, CAS registry no. 98-95-3), and phenol (C_6H_6O, assay ≥ 99.5 %, Lot and filling code 1373574 21308237, CAS registry no. 108-95-2) were obtained from Aldrich/Fluka (Buchs, Switzerland). 1,2,3-Trimethylbenzene (hemimellitene or hemellitol, C_9H_{12}, assay 98 %, Catalog and Lot no. 8776.05 8776.05-5, CAS registry no. 526-73-8) was obtained from ChemSampCo (Trenton, NJ). The substituted benzenes were used without further purification.

The ionic liquid 1-ethyl-3-methylimidazolium bis(trifluoromethylsulfonyl)imide [emim][Tf_2N] (electrochemical grade, assay ≥ 99.5 %, $C_8H_{11}F_6N_3O_4S_2$, Lot and Catalog no. 259095 IL-201-20-E, CAS registry no. 174899-82-2) was purchased from Covalent Associates Inc. (Corvallis, OR). Figure 1 provides the chemical structure and molar mass. Elemental analysis was used to check the purity of the [emim][Tf_2N] sample. The purity was ≥ 99.4 %, and a detailed description of the analysis can be found in our previous work.[9] The [emim][Tf_2N] was dried and degassed by filling a borosilicate glass tube with about 10 g of the ionic liquid and pulling a coarse vacuum with a diaphragm

---

* Corresponding author. E-mail: mark.b.shiflett@usa.dupont.com.

10.1021/je9003614 CCC: $40.75

Chemical Name	Abbreviation	Structure
1-ethyl-3-methylimidazolium bis(trifluoromethylsulfonyl)imide	[emim][Tf$_2$N]	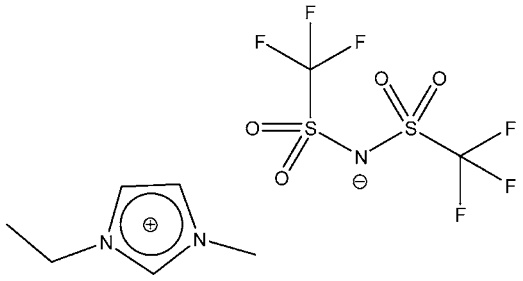

Figure 1. Schematic molecular structure and abbreviation of 1-ethyl-3-methylimidazolium bis(trifluoromethylsulfonyl)imide. Molar mass: 391.31 g·mol^{-1}.

pump (Pfeiffer, model MVP055-3, Nashua, NH) followed by further evacuation using a turbopump (Pfeiffer, model TSH-071) to a pressure of about $4 \cdot 10^{-7}$ kPa while simultaneously heating and stirring the ionic liquid at a temperature of about 348 K for 5 days. The final water mass fraction was measured by Karl Fischer titration (AquaStar C3000, solution AquaStar Coulomat C and A), and the dried sample contained $188 \cdot 10^{-6}$ H_2O.

Experimental Method. Detailed descriptions of the LLE experimental equipment and procedures are available in our previous reports.[13,14] Therefore, only the basic experimental techniques and measurement uncertainties are given here. LLE measurements were made with samples containing mole fractions of (70 and 90) % substituted benzenes + [emim][Tf$_2$N] at constant temperatures from about (293 to 373) K using the volumetric method.[13,14]

To measure LLE over a wide range of temperatures, two thermostat baths were utilized. A water-filled thermostat bath was used for measurements between temperatures of (293 and 333) K. Higher temperature measurements at (353 to 373) K were performed using a silicone oil-filled thermostat bath (Tamson Instruments, TV4000LT, Zoetermeer, Netherlands). The uncertainty in temperature for both thermostat baths was ± 0.2 K and was determined using a standard platinum resistance thermometer [SPRT model 5699, Hart Scientific, American Fork, UT, range (73 to 933) K] and readout (Blackstack model 1560 with SPRT module 2560) with a NIST certified traceable accuracy to ± 0.005 K.

Results

Experimental Data. To use the mass−volume method,[13,14] the vapor phase was assumed to contain only substituted benzenes (negligible vapor pressure for [emim][Tf$_2$N] ionic liquid). The vapor density for toluene was calculated using the REFPROP computer program.[35] The vapor densities for ethylbenzene, propylbenzene, (*ortho*, *meta*, *para*)-xylene, and (1,2,3, 1,2,4, 1,3,5)-trimethylbenzene were calculated assuming ideal gas behavior and known vapor pressure data.[36] The total uncertainties were estimated by calculating both the overall random and systematic uncertainties. The following experimental parameters were considered to have an effect on the random uncertainty: sample container volume calibration, mass of substituted benzenes and ionic liquid, and the heights of the lower and upper phases. The heights had the largest overall effect. The systematic uncertainties include properly correcting for the area expansion, meniscus, and vapor phase moles. For additional details on estimation of total uncertainties, see refs 13 and 14. Total uncertainties in the final composition and molar volume are provided in Table 1.

One of the advantages of using the present method is the ability to obtain the molar volume of each separated liquid simultaneously with the composition of each liquid at any given isothermal condition. Then, the excess molar volume of each liquid solution ($V^{E'}$ and V^{E}) can be obtained, by use of the pure component molar volumes V_1^0 (substituted benzenes) and V_2^0 ([emim][Tf$_2$N]) using

$$V^{E'} = V_m - x'_1 V_1^0 - x'_2 V_2^0 \text{ or } V^{E} = V_m - x_1 V_1^0 - x_2 V_2^0 \tag{1}$$

where V_m is the measured molar volume of the mixture ($V_m = V'$ for the lower phase L′ *or* $V_m = V$ for the upper phase L), and (x'_1, x'_2 or x_1, x_2) are mole fractions of substituted benzenes (1) and ionic liquid (2) in phase L′ or L, respectively. Saturated liquid molar volumes for toluene were calculated using the REFPROP computer program.[35] Saturated liquid molar volumes for all other substituted benzenes were calculated using the modified Rackett technique and measured liquid density data provided in ref 36. Saturated liquid molar volumes for [emim][Tf$_2$N] were calculated using liquid density data measured by Krummen et al.[37]

Thermodynamic Model Analysis. Liquid−liquid equilibria for an N-component system at low pressures can be described by the following set of nonlinear equations with liquid mole fractions, x_i, and activity coefficients, γ_i[38]

$$\gamma_i^{L1} x_i^{L1} = \gamma_i^{L2} x_i^{L2} \quad (i = 1,...,N) \tag{2}$$

where $N = 2$ for a binary system; superscripts L1 and L2 indicate two liquid phases of LLE; and $i = 1$ designates species 1 (substituted benzenes), while $i = 2$ corresponds to species 2, the ionic liquid [emim][Tf$_2$N]. For the activity coefficient, we use the NRTL (nonrandom two liquids) solution model.[36]

Table 1. (a) Toluene (1) + [emim][Tf$_2$N] (2) System, (b) Ethylbenzene (1) + [emim][Tf$_2$N] (2) System, (c) Propylbenzene (1) + [emim][Tf$_2$N] (2) System, (d) *ortho*-Xylene (1) + [emim][Tf$_2$N] (2) System, (e) *meta*-Xylene (1) + [emim][Tf$_2$N] (2) System, (f) *para*-Xylene (1) + [emim][Tf$_2$N] (2) System, (g) 1,2,3-Trimethylbenzene (1) + [emim][Tf$_2$N] (2) System, (h) 1,2,4-Trimethylbenzene (1) + [emim][Tf$_2$N] (2) System, and (i) 1,3,5-Trimethybenzene (1) + [emim][Tf$_2$N] (2) System[a]

(a)			V'	V	$V^{E'}$	V^E
T/K	$100x'_1$	$100x_1$	cm^3·mol^{-1}	cm^3·mol^{-1}	cm^3·mol^{-1}	cm^3·mol^{-1}
297.7 ± 0.2	65.6 ± 0.2	100.0 − 0.2	155.7 ± 1.3	105.9 ± 0.5	−2.9 ± 1.3	−0.2 ± 0.5
314.2 ± 0.2	64.9 ± 0.2	100.0 − 0.2	158.8 ± 1.3	107.6 ± 0.5	−3.2 ± 1.3	−0.5 ± 0.5
334.2 ± 0.2	64.0 ± 0.3	100.0 − 0.2	162.6 ± 1.6	110.0 ± 0.5	−3.5 ± 1.6	−0.6 ± 0.5
353.1 ± 0.2	63.6 ± 0.3	100.0 − 0.2	164.7 ± 2.2	112.6 ± 0.6	−4.9 ± 2.2	−0.7 ± 0.6
372.9 ± 0.2	63.1 ± 0.2	100.0 − 0.2	167.9 ± 1.3	115.7 ± 0.5	−5.7 ± 1.3	−0.4 ± 0.5

(b)			V'	V	$V^{E'}$	V^E
T/K	$100x'_1$	$100x_1$	cm^3·mol^{-1}	cm^3·mol^{-1}	cm^3·mol^{-1}	cm^3·mol^{-1}
293.4 ± 0.2	51.5 ± 0.4	100.0 − 0.2	186.0 ± 1.6	121.4 ± 0.6	−1.6 ± 1.6	−0.8 ± 0.6
314.0 ± 0.2	50.5 ± 0.3	100.0 − 0.2	191.1 ± 1.8	123.7 ± 0.6	−1.9 ± 1.8	−1.1 ± 0.6
333.9 ± 0.2	50.4 ± 0.3	100.0 − 0.2	193.3 ± 1.5	126.5 ± 0.8	−1.9 ± 1.5	−1.0 ± 0.8
353.1 ± 0.2	50.1 ± 0.3	100.0 − 0.2	196.3 ± 1.4	129.1 ± 0.6	−2.4 ± 1.4	−1.1 ± 0.6
373.0 ± 0.2	49.8 ± 0.3	100.0 − 0.2	199.7 ± 1.4	131.7 ± 0.6	−2.8 ± 1.4	−1.0 ± 0.6

(c)			V'	V	$V^{E'}$	V^E
T/K	$100x'_1$	$100x_1$	cm^3·mol^{-1}	cm^3·mol^{-1}	cm^3·mol^{-1}	cm^3·mol^{-1}
293.1 ± 0.2	36.1 ± 0.4	100.0 − 0.2	212.0 ± 1.2	138.2 ± 0.6	−2.5 ± 1.2	−0.7 ± 0.6
313.9 ± 0.2	35.7 ± 0.4	100.0 − 0.2	215.7 ± 1.2	141.1 ± 0.7	−2.4 ± 1.2	−0.6 ± 0.7
333.9 ± 0.2	35.1 ± 0.4	100.0 − 0.2	221.4 ± 1.2	144.0 ± 0.7	−1.0 ± 1.2	−0.7 ± 0.7
353.1 ± 0.2	34.9 ± 0.5	100.0 − 0.2	225.2 ± 2.9	147.5 ± 0.7	−0.3 ± 2.9	−0.4 ± 0.7
373.0 ± 0.2	34.8 ± 0.5	100.0 − 0.2	229.4 ± 2.9	150.2 ± 0.7	−0.2 ± 2.9	−0.8 ± 0.7

(d)			V'	V	$V^{E'}$	V^E
T/K	$100x'_1$	$100x_1$	cm^3·mol^{-1}	cm^3·mol^{-1}	cm^3·mol^{-1}	cm^3·mol^{-1}
297.7 ± 0.2	55.6 ± 0.5	100.0 − 0.2	177.1 ± 1.7	121.0 ± 1.1	−4.6 ± 1.7	−0.2 ± 1.1
314.2 ± 0.2	54.9 ± 0.5	100.0 − 0.2	180.1 ± 1.6	122.7 ± 1.1	−5.1 ± 1.6	−0.5 ± 1.1
334.2 ± 0.2	54.8 ± 0.5	100.0 − 0.2	182.6 ± 1.8	125.2 ± 1.0	−5.4 ± 1.8	−0.5 ± 1.0
353.1 ± 0.2	54.4 ± 0.8	100.0 − 0.2	187.7 ± 1.8	127.7 ± 1.4	−4.1 ± 1.8	−0.8 ± 1.4
372.9 ± 0.2	53.9 ± 0.8	100.0 − 0.2	191.5 ± 1.9	130.5 ± 1.4	−4.1 ± 1.9	−0.8 ± 1.4

(e)			V'	V	$V^{E'}$	V^E
T/K	$100x'_1$	$100x_1$	cm^3·mol^{-1}	cm^3·mol^{-1}	cm^3·mol^{-1}	cm^3·mol^{-1}
297.7 ± 0.2	50.2 ± 0.5	100.0 − 0.2	186.6 ± 1.9	122.3 ± 1.1	−3.6 ± 1.9	−1.2 ± 1.1
314.2 ± 0.2	49.8 ± 0.5	100.0 − 0.2	188.7 ± 1.2	124.5 ± 1.3	−4.5 ± 1.2	−1.0 ± 1.3
334.2 ± 0.2	49.3 ± 0.5	100.0 − 0.2	192.2 ± 1.0	127.2 ± 1.5	−4.8 ± 1.0	−1.0 ± 1.5
353.1 ± 0.2	48.3 ± 0.5	100.0 − 0.2	197.1 ± 1.9	130.4 ± 2.1	−4.4 ± 1.9	−0.5 ± 2.1
372.9 ± 0.2	48.1 ± 1.0	100.0 − 0.2	200.5 ± 2.0	132.8 ± 2.0	−4.5 ± 2.0	−1.1 ± 2.0

(f)			V'	V	$V^{E'}$	V^E
T/K	$100x'_1$	$100x_1$	cm^3·mol^{-1}	cm^3·mol^{-1}	cm^3·mol^{-1}	cm^3·mol^{-1}
297.7 ± 0.2	49.1 ± 0.5	100.0 − 0.2	191.7 ± 2.0	123.5 ± 1.2	−1.2 ± 2.0	−0.4 ± 1.2
314.2 ± 0.2	48.6 ± 0.5	100.0 − 0.2	194.7 ± 2.0	125.7 ± 1.2	−1.3 ± 2.0	−0.3 ± 1.2
334.2 ± 0.2	48.0 ± 0.6	100.0 − 0.2	198.4 ± 2.1	128.4 ± 1.2	−1.6 ± 2.1	−0.3 ± 1.2
353.1 ± 0.2	47.6 ± 1.1	100.0 − 0.2	201.3 ± 2.2	131.6 ± 1.4	−1.9 ± 2.2	−0.2 ± 1.4
372.9 ± 0.2	47.5 ± 1.1	100.0 − 0.2	203.5 ± 2.6	134.4 ± 1.5	−2.5 ± 2.6	−0.2 ± 1.5

(g)			V'	V	$V^{E'}$	V^E
T/K	$100x'_1$	$100x_1$	cm^3·mol^{-1}	cm^3·mol^{-1}	cm^3·mol^{-1}	cm^3·mol^{-1}
292.7 ± 0.2	42.4 ± 0.6	100.0 − 0.2	200.0 ± 1.9	133.7 ± 0.7	−4.9 ± 1.9	−0.8 ± 0.7
314.1 ± 0.2	41.3 ± 0.6	100.0 − 0.2	204.6 ± 1.5	136.1 ± 0.7	−4.8 ± 1.5	−0.9 ± 0.7
334.0 ± 0.2	41.5 ± 0.6	100.0 − 0.2	206.1 ± 1.4	139.4 ± 0.7	−5.3 ± 1.4	−0.2 ± 0.7
353.1 ± 0.2	42.1 ± 0.8	100.0 − 0.2	207.7 ± 1.6	142.0 ± 0.8	−4.9 ± 1.6	−0.4 ± 0.8
373.0 ± 0.2	41.9 ± 0.8	100.0 − 0.2	212.1 ± 1.6	144.3 ± 0.8	−5.1 ± 1.6	−0.8 ± 0.8

(h)			V'	V	$V^{E'}$	V^E
T/K	$100x'_1$	$100x_1$	cm^3·mol^{-1}	cm^3·mol^{-1}	cm^3·mol^{-1}	cm^3·mol^{-1}
293.8 ± 0.2	36.2 ± 0.5	100.0 − 0.2	213.7 ± 1.5	136.2 ± 0.7	−1.2 ± 1.5	−1.0 ± 0.7
313.9 ± 0.2	35.5 ± 0.7	100.0 − 0.2	217.4 ± 1.5	138.8 ± 0.7	−1.1 ± 1.5	−1.0 ± 0.7
333.7 ± 0.2	35.2 ± 0.7	100.0 − 0.2	220.0 ± 1.6	141.5 ± 0.7	−1.1 ± 1.6	−1.0 ± 0.7
353.1 ± 0.2	35.9 ± 0.7	100.0 − 0.2	221.6 ± 1.7	144.0 ± 0.8	−1.9 ± 1.7	−1.3 ± 0.8
373.0 ± 0.2	36.0 ± 0.7	100.0 − 0.2	225.3 ± 1.6	146.9 ± 0.8	−1.6 ± 1.6	−1.3 ± 0.8

(i)			V'	V	$V^{E'}$	V^E
T/K	$100x'_1$	$100x_1$	cm^3·mol^{-1}	cm^3·mol^{-1}	cm^3·mol^{-1}	cm^3·mol^{-1}
292.7 ± 0.2	30.5 ± 0.7	100.0 − 0.2	220.9 ± 1.9	137.2 ± 0.7	−1.2 ± 1.9	−0.7 ± 0.7
314.1 ± 0.2	30.7 ± 0.7	100.0 − 0.2	223.2 ± 2.2	140.3 ± 0.7	−1.2 ± 2.2	−0.5 ± 0.7
334.0 ± 0.2	31.7 ± 0.7	100.0 − 0.2	225.5 ± 1.6	143.7 ± 0.7	−1.8 ± 1.6	−1.0 ± 0.7
353.1 ± 0.2	31.9 ± 0.7	100.0 − 0.2	228.1 ± 2.1	146.3 ± 0.8	−1.8 ± 2.1	−1.0 ± 0.8
373.0 ± 0.2	32.3 ± 0.7	100.0 − 0.2	229.7 ± 1.6	149.2 ± 0.8	−2.5 ± 1.6	−1.0 ± 0.8

[a] x'_1, observed molar composition lower phase; x_1, observed molar composition upper phase; V', observed molar volume lower phase; V, observed molar volume upper phase; $V^{E'}$, excess molar volume lower phase; V^E, excess molar volume upper phase.

Table 2. NRTL Binary Interaction Parameters in Equation 7

compound (1) in [emim][Tf$_2$N] (2)	$\tau_{12}^{(0)}$	$\tau_{12}^{(1)}$/K	$\tau_{21}^{(0)}$	$\tau_{21}^{(1)}$/K
toluene	7.9825	246.50	−1.4184	−226.18
ethylbenzene	7.6376	103.19	−1.0399	−104.11
propylbenzene	7.0534	76.72	−0.3866	−86.42
ortho-xylene	7.8026	119.94	−1.2137	−117.58
meta-xylene	7.3983	161.38	−0.7931	−164.45
para-xylene	7.4886	116.28	−0.8829	−119.21
1,2,3-trimethylbenzene	7.5275	9.47	−0.9148	−10.11
1,2,4-trimethylbenzene	7.2913	3.88	−0.6546	−4.35
1,3,5-trimethylbenzene	7.4440	−104.22	−0.8355	121.37

The binary activity coefficients of the NRTL model are given by

$$\ln \gamma_1 = x_2^2\left[\tau_{21}\left(\frac{G_{21}}{x_1 + x_2 G_{21}}\right)^2 + \frac{\tau_{12}G_{12}}{(x_2 + x_1 G_{12})^2}\right] \quad (3)$$

$$\ln \gamma_2 = x_1^2\left[\tau_{12}\left(\frac{G_{12}}{x_2 + x_1 G_{12}}\right)^2 + \frac{\tau_{21}G_{21}}{(x_1 + x_2 G_{21})^2}\right] \quad (4)$$

where

$$G_{12} \equiv \exp(-\alpha\tau_{12}) \text{ and } G_{21} \equiv \exp(-\alpha\tau_{21}) \quad (5)$$

$$\tau_{12} \equiv \frac{\Delta g_1}{RT} \text{ and } \tau_{21} \equiv \frac{\Delta g_2}{RT} \text{ (adjustable binary interaction parameters),} \quad (6)$$

$\alpha = 0.2$ (assumed to be a constant of 0.2 in this work), and x_i = mole fraction of the *i*th species.

The temperature-dependent binary interaction parameter (τ_{ij}) is modeled here by a two-term empirical equation

$$\tau_{12} = \tau_{12}^{(0)} + \tau_{12}^{(1)}/(T/\text{K}) \text{ and } \tau_{21} = \tau_{21}^{(0)} + \tau_{21}^{(1)}/(T/\text{K}) \quad (7)$$

Then, the two unknown adjustable parameters τ_{12} and τ_{21} at a given T can be determined from *one* set of LLE experimental (the present volumetric method) data, using eq 2 (two nonlinearly coupled equations). We have five sets of such LLE data for each binary system, as shown in Table 1, and can obtain a set of τ_{12} and τ_{21} at each respective temperature. Thus, the four empirical parameters in eq 7 have been determined from the obtained τ_{ij} data and are given in Table 2.

Once the binary interaction parameters of the NRTL model have been determined as a function of temperature, we can calculate the *Tx* (temperature−composition) phase diagram at any temperature by solving eq 2. Numerical solutions of eq 2 have been obtained by use of a robust flash algorithm.[38] Calculated *Tx* diagrams for the present LLE systems were successfully constructed and compared well with the experimental solubility data as shown in Figures 2 to 4.

Discussion

We have continued our evaluation of the phase behavior of alkyl-substituted benzenes (C_7H_8, C_8H_{10}-isomers, C_9H_{12}-isomers) and nonalkyl-substituted benzenes ($-NH_2$, $-NO_2$, $-OH$, $-CHO$) with RTIL, [emim][Tf$_2$N], to provide some insight on these molecular interactions compared with our original work on fluorinated ($C_6H_nF_{6-n}$: $n = 1,...,5$)[5,6] and other halogenated benzenes (C_6H_5X where X = Cl, Br, I)[7] with [emim][Tf$_2$N]. In our previous works,[5−7] we showed that the polarity and the molecular size of the solute (substituted benzene) played an important role in determining the solubility in the solvent (RTIL). The polarity of RTILs is an area of current research interest. Both solvatochromic and fluorescent dyes have been utilized to determine the polarity of these molten salts, and different combinations of cations and anions lead to solvents with different polarities.[39−45] In the case of [emim][Tf$_2$N], both the cation and anion have dipole moments, and the molecule is considered to be polar. This leads the novice to the typical association rule of "like dissolves like" suggesting that for a substituted benzene a larger dipole moment leads to a greater degree of solubility in the RTIL ([emim][Tf$_2$N]). In some cases this is true, but the solute molecular size also plays an important role in determining the degree of solubility.

Figure 2 provides the phase diagrams (*Tx*) for the binary systems toluene (methylbenzene), ethylbenzene, and propylbenzene + [emim][Tf$_2$N]. The binary pair of benzene + [emim][Tf$_2$N] from our previous work[5] has also been included for comparison. The mole fraction immiscibility gaps ($\Delta 100 x_1$) at 298 K for benzene, toluene, ethylbenzene, and propylbenzene in [emim][Tf$_2$N] are about (23, 34, 49 and 64) %, respectively. The dipole moments for benzene, toluene, ethylbenzene, and propylbenzene are (0, 0.4, 0.4, and 0.4) D ($1\ \text{D} = 3.33564 \cdot 10^{-30}$ C·m).[36,46] The measured immiscibility gap does not correlate with the solute dipole moment.

For an explanation of the immiscibility gap, we compared the molecular size of the solute. As the solute molecular size increased (benzene < methylbenzene < ethylbenzene < propylbenzene) with the length of the alkyl side chain, the immiscibility gap also increased. One explanation using molecular dynamic calculations by Huang et al.[47] for the binary system (CO_2 + [bmim][PF$_6$]) indicates that small angular rearrangements of the anion can occur which create localized cavities where molecules can fit above and below the imidazolium ring. In this case, angular rearrangements of the [Tf$_2$N] anion must create cavities where the alkyl-substituted benzenes can fit around the [emim] cation. The size of the solute determines the amount of the substituted benzene which can fill these cavities and exist in the ionic liquid-rich phase. As the solute molecular size increases, less solute can fill these cavities resulting in the increase in the immiscibility gap. As discussed in our previous work,[5−7] when the solutes (substituted benzenes) have similar polarities, other factors such as molecular size become important.

Figure 3 provides the phase diagrams (*Tx*) for the binary systems 1,2-dimethylbenzene (*o*-xylene), 1,3-dimethylbenzene (*m*-xylene), and 1,4-dimethylbenzene (*p*-xylene) + [emim][Tf$_2$N]. The mole fraction immiscibility gaps ($\Delta 100 x_1$) at 298 K for *o*-xylene, *m*-xylene, and *p*-xylene in [emim][Tf$_2$N] are about (44, 50, and 51) %, respectively. In this case the immiscibility gap increases as the dipole moment decreases (i.e., immiscibility gap correlates with the dipole moment). The dipole moments for *o*-xylene, *m*-xylene, and *p*-xylene are (0.5, 0.3, and 0.1) D, respectively.[36,46] The immiscibility gap also correlates with the maximum molecular size of the solute (*o*-xylene < *m*-xylene < *p*-xylene).[48]

Figure 4 provides the phase diagrams (*Tx*) for the binary systems 1,2,3-trimethylbenzene (hemimellitene), 1,2,4-trimethylbenzene (pseudocumene), and 1,3,5-trimethylbenzene (mesitylene) + [emim][Tf$_2$N]. The mole fraction immiscibility gaps ($\Delta 100 x_1$) at 298 K for (1,2,3; 1,2,4; and 1,3,5)-trimethylbenzene in [emim][Tf$_2$N] are about (58, 63, and 67) %, respectively. The measured immiscibility gap correlates with the solute dipole moment. The dipole moments for (1,2,3; 1,2,4; and 1,3,5)-trimethylbenzene are (0.6, 0.3, and 0.1) D, respectively.[36,46] Similar to that of the xylene isomers, the immiscibility gap also

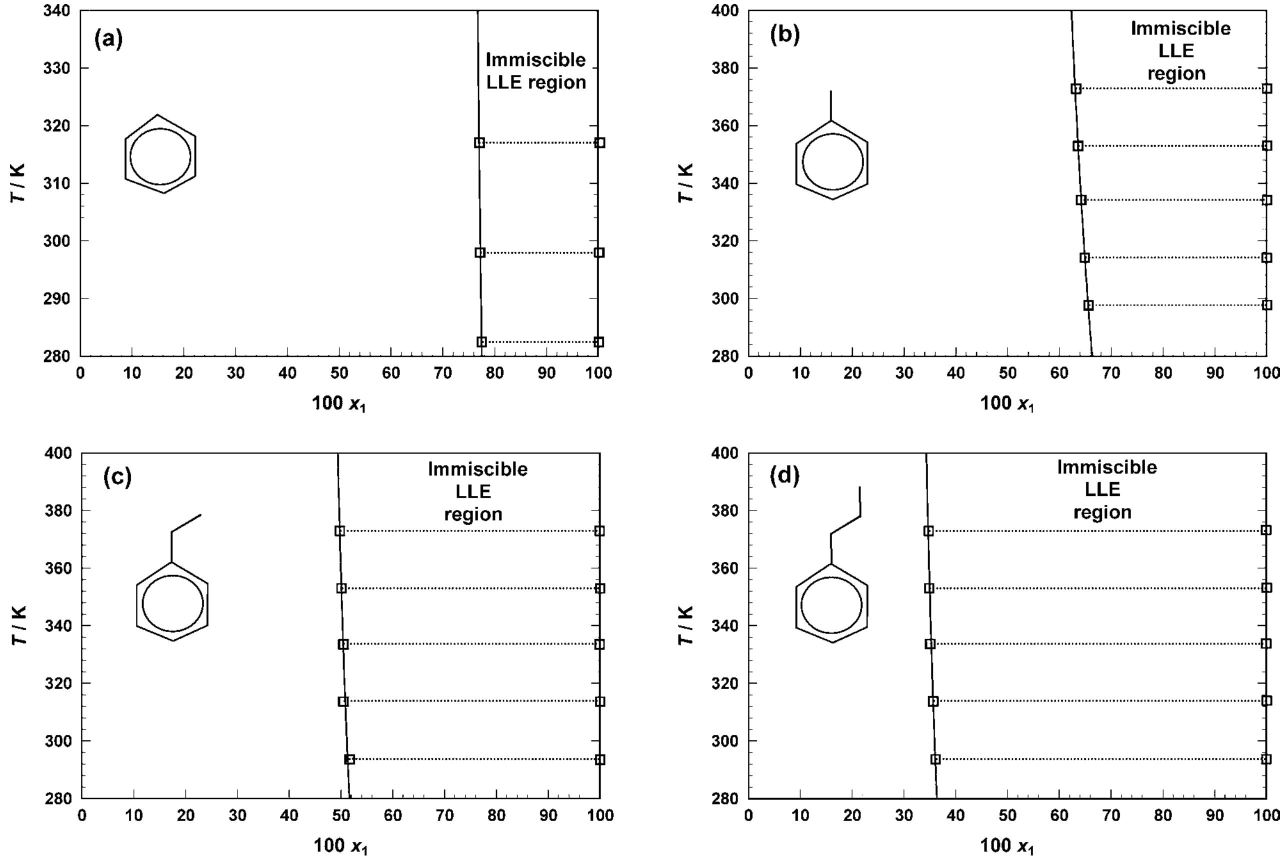

Figure 2. *Tx* phase diagrams for LLE of (a) benzene (1) + [emim][Tf_2N] (2), taken from ref 5; (b) toluene (1) + [emim][Tf_2N] (2); (c) ethylbenzene (1) + [emim][Tf_2N] (2); and (d) propylbenzene (1) + [emim][Tf_2N] (2). Solid line: the NRTL model calculation. Broken lines: experimental LLE tie lines. Symbols: □, experimental data by the volumetric method.

correlates with the maximum molecular size of the solute (1,2,3-trimethylbenzene < 1,2,4-trimethylbenzene < 1,3,5-trimethylbenzene).[48]

Furthermore, a comparison of the mole fraction immiscibility gap ($\Delta 100x_1$) at 298 K for C_6H_6 about 23 %, C_7H_8 about 34 %, C_8H_{10}-isomers about (44 to 51) %, and C_9H_{12}-isomers about (58 to 67) % shows a correlation with molecular size which is independent of polarity.

The phase behaviors for nonalkyl-substituted benzenes (phenol, aniline, benzaldehyde, and nitrobenzene) were also measured in RTIL ([emim][Tf_2N]). Unexpectedly, we have found that all four of these nonalkyl-substituted benzenes were soluble for samples containing mole fractions of (70 and 90) % at constant temperatures from about (293 to 373) K. Additional samples with compositions containing nonalkyl-substituted benzene mole fractions from (1 to 99) % were prepared, and aniline, nitrobenzene, and benzaldehyde were completely soluble in RTIL ([emim][Tf_2N]) over the temperature range from about (293 to 373) K. Phenol, which is a solid at room temperature, dissolves in RTIL ([emim][Tf_2N] when heated to about 323 K and remains a single liquid phase upon cooling to 293 K for mixtures containing mole fractions from (1 to 90) % phenol. Therefore, the choice of functional group on the benzene ring (−OH, $-NH_2$, −CHO, and $-NO_2$) affects the solute's ability to dissolve in a RTIL ([emim][Tf_2N]). The dipole moments for phenol, aniline, benzaldehyde, and nitrobenzene are (1.4, 1.5, 3.0, and 4.2) D, respectively.[49] In the present work, we have shown that both the solute polarity and molecular size play an important role in controlling the miscibility in RTIL ([emim][Tf_2N]) and may be the most dominant effects.

However, we have presented examples in our previous work for binary mixtures containing hydrofluorocarbons (HFCs) and RTILs that show no correlation between dipole moment and miscibility in RTILs.[9,14,17] In the case of HFCs, additional intermolecular interactions may be playing a role such as the unique hydrogen-bonding capability (H−F−H) between fluorinated compounds and ionic liquids. In addition, other interactions such as higher-order moments (quadrupole, octupole)[50−52] and π-electron (π-cation and π-anion) effects[50,53−55] may also be important. The unique interactions between substituted benzene molecules in ionic liquids continue to pose a unique and interesting challenge for theoretical modelers.

The present LLE data have been well correlated with the nonelectrolyte NRTL solution model. In the present case, as the temperature increases, the immiscibility gap widens as shown in Figures 2 and 3 or remains essentially constant as shown in Figure 4, and the LLE behavior is similar to other substituted benzenes (fluorinated benzenes) we have measured in [emim][Tf_2N].[6] The present volumetric method for LLE also provides information for the liquid molar volume and excess molar volume for each liquid phase. In the present work, the substituted benzene-rich phase contains a mole fraction of (99.8 to 100.0) % substituted benzene with an excess molar volume from about (0 to −1) $cm^3 \cdot mol^{-1}$. The [emim][Tf_2N]-rich phase has an excess molar volume from about (−1 to −5) $cm^3 \cdot mol^{-1}$. In ordinary binary mixtures,[56,57] the excess molar volume is at most ± (1 to 2) $cm^3 \cdot mol^{-1}$; therefore, like various HFC mixtures with RTILs,[13−15] these mixtures do not behave ideally. Such information provides new insights on the physical structures in the liquid solutions containing RTILs.

Conclusions

The phase behavior in binary mixtures of substituted benzenes (toluene, ethylbenzene, propylbenzene, dimethylbenzene iso-

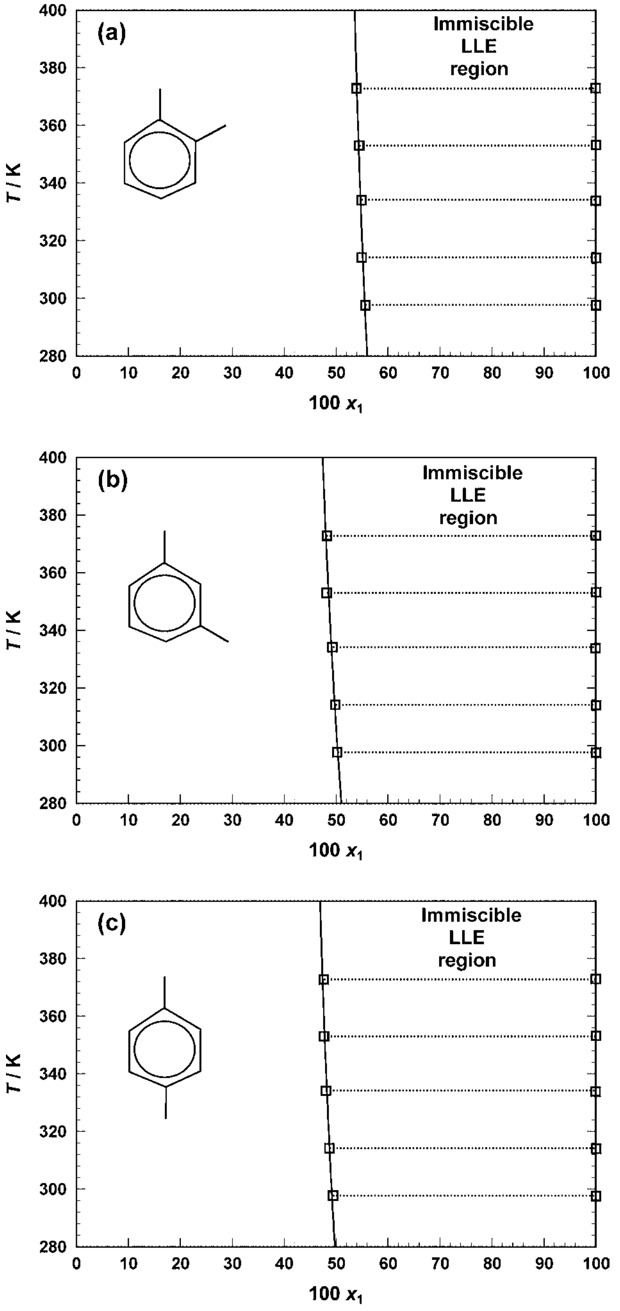

Figure 3. *Tx* phase diagrams for LLE of (a) *ortho*-xylene (1) + [emim][Tf_2N] (2); (b) *meta*-xylene (1) + [emim][Tf_2N] (2); and (c) *para*-xylene (1) + [emim][Tf_2N] (2). Solid line: the NRTL model calculation. Broken lines: experimental LLE tie lines. Symbols: □, experimental data by the volumetric method.

mers, trimethylbenzene isomers, aniline, nitrobenzene, phenol, and benzaldehyde) with RTIL [emim][Tf_2N] have been measured with the volumetric method. A trend in the miscibility with polarity and molecular size of the solute was found. In general, as the polarity increased and the molecular size decreased, the immiscibility gap became smaller. The smaller size allows more of the solute to exist in localized cavities above and below the imidazolium ring. As the solute molecular size increases (e.g., methybenzene < ethylbenzene < propylbenzene), less of the solute can fill these cavities, resulting in a larger immiscibility region. In the case of dimethylbenzene and trimethylbenzene isomers, as the polarity increased and the molecular size decreased, the immiscibility gap became smaller. The nonalkyl-substituted benzenes containing functional groups

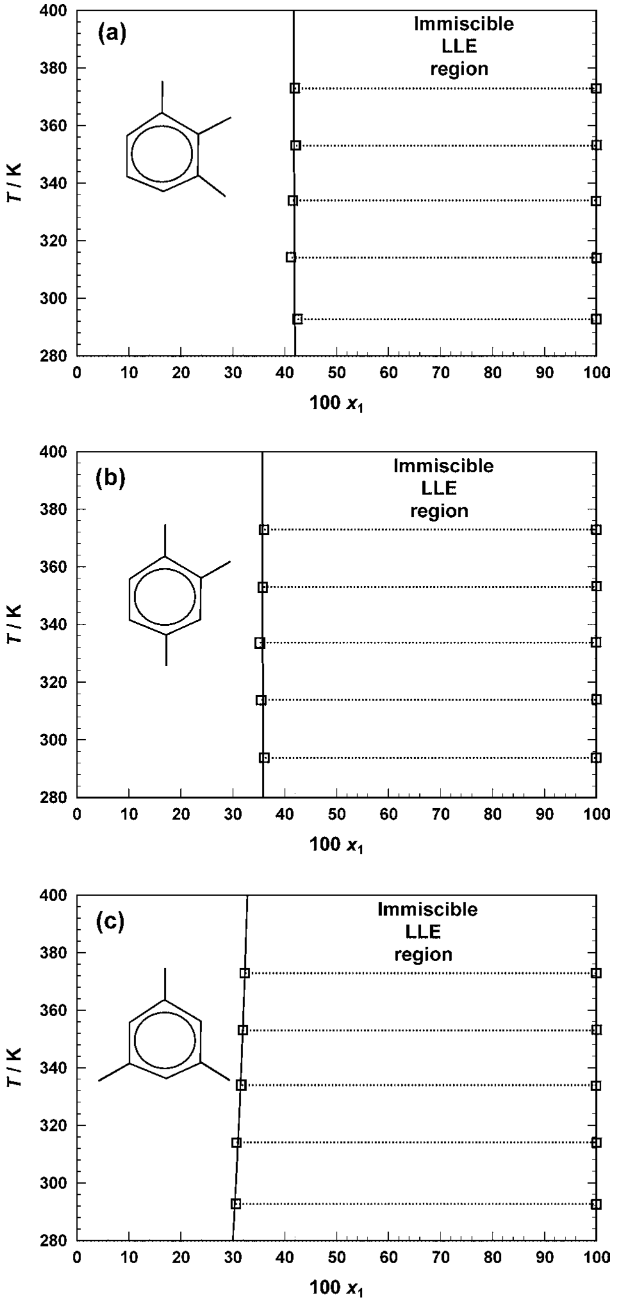

Figure 4. *Tx* phase diagrams for LLE of (a) 1,2,3-trimethylbenzene (1) + [emim][Tf_2N] (2); (b) 1,2,4-trimethylbenzene (1) + [emim][Tf_2N] (2); and (c) 1,3,5-trimethylbenzene (1) + [emim][Tf_2N] (2). Solid line: the NRTL model calculation. Broken lines: experimental LLE tie lines. Symbols: □, experimental data by the volumetric method.

($-NH_2$, $-NO_2$, $-OH$, and $-CHO$) were completely soluble in [emim][Tf_2N] over the composition and temperature range studied. LLE data are well correlated with the nonelectrolyte NRTL model, and the negative excess molar volumes in the ionic liquid-rich side solutions range from about (−1 to −5) $cm^3 \cdot mol^{-1}$.

Acknowledgment

The authors gratefully acknowledge Dr. Akimichi Yokozeki for providing his computer models used in the analysis of the liquid−liquid equilibrium data and for his valuable ideas, discussion, and teaching that richly contributed to this paper.

Literature Cited

(1) Wasserschheid, P.; Welton, T., Eds. *Ionic Liquids in Synthesis*; Wiley-VCH: Weinheim, Germany, 2003.

(2) Zhao, H. Innovative Applications of Ionic Liquids as "Green" Engineering Liquids. *Chem. Eng. Commun.* **2006**, *193*, 1660–1677.
(3) Plechkova, N. V.; Seddon, K. R. Applications of ionic liquids in the chemical industry. *Chem. Soc. Rev.* **2008**, *37*, 123–150.
(4) NIST Ionic Liquid Database; http://ilthermo.boulder.nist.gov, 2006.
(5) Yokozeki, A.; Shiflett, M. B. Binary and Ternary Phase Diagrams of Benzene, Hexafluorobenzene, and Ionic Liquid [emim][Tf$_2$N] using Equations of State. *Ind. Eng. Chem. Res.* **2008**, *47*, 8389–8395.
(6) Shiflett, M. B.; Yokozeki, A. Liquid-Liquid Equilibria in Binary Mixtures containing Fluorinated Benzenes and Ionic Liquid 1-ethyl-3-methylimidazolium bis(trifluoromethylsulfonyl)imide. *J. Chem. Eng. Data* **2008**, *53*, 2683–2691.
(7) Shiflett, M. B.; Niehaus, A. M. S.; Yokozeki, A. Liquid-Liquid Equilibria in Binary Mixtures containing Chlorobenzene, Bromobenzene, and Iodobenzene with Ionic Liquid 1-ethyl-3-methylimidazolium bis(trifluoromethylsulfonyl)imide. *J. Chem. Eng. Data* **2009**, DOI: 10.1021/je801005y.
(8) Shiflett, M. B.; Yokozeki, A. Solubility and Diffusivity of Hydrofluorocarbons in Room-Temperature Ionic Liquids. *AIChE J.* **2006**, *52*, 1205–1219.
(9) Shiflett, M. B.; Yokozeki, A. Solubility Differences of Halocarbon Isomers in Ionic Liquid [emim][Tf$_2$N]. *J. Chem. Eng. Data* **2007**, *52*, 2007–2015.
(10) Shiflett, M. B.; Junk, C. P.; Harmer, M. A.; Yokozeki, A. Solubility and Diffusivity of Difluoromethane in Room-Temperature Ionic Liquids. *J. Chem. Eng. Data* **2006**, *51*, 483–495.
(11) Shiflett, M. B.; Junk, C. P.; Harmer, M. A.; Yokozeki, A. Solubility and Diffusivity of 1,1,1,2-tetrafluoroethane in Room-Temperature Ionic Liquids. *Fluid Phase Equilib.* **2006**, *242*, 220–232.
(12) Shiflett, M. B.; Yokozeki, A. Gaseous Absorption of Fluoromethane, Fluoroethane, and 1,1,2,2-Tetrafluoroethane in 1-butyl-3-methylimidazolium Hexafluorophosphate. *Ind. Chem. Eng. Res.* **2006**, *45*, 6375–6382.
(13) Shiflett, M. B.; Yokozeki, A. Vapor-Liquid-Liquid Equilibria of Pentafluoroethane and Ionic Liquid [bmim][PF$_6$] Mixtures studied with the Volumetric Method. *J. Phys. Chem. B* **2006**, *110*, 14436–14443.
(14) Shiflett, M. B.; Yokozeki, A. Vapor-Liquid-Liquid Equilibria of Hydrofluorocarbons and 1-Butyl-3-Methylimidazolium Hexafluorophosphate. *J. Chem. Eng. Data* **2006**, *51*, 1931–1939.
(15) Yokozeki, A.; Shiflett, M. B. Global Phase Behaviors of Trifluoromethane in Room-Temperature Ionic Liquid [bmim][PF$_6$]. *AIChE J.* **2006**, *52*, 3952–3957.
(16) Shiflett, M. B.; Yokozeki, A. Phase Equilibria of Hydrofluorocarbon-4310mee Mixtures with Ionic Liquids: Miscibility of Threo- and Erythro-Diastereomers in Ionic Liquids. *Ind. Eng. Chem. Res.* **2008**, *47*, 926–934.
(17) Shiflett, M. B.; Yokozeki, A. Hydrogen Substitution Effect on the Solubility of Perhalogenated Compounds in Ionic Liquid [bmim][PF$_6$]. *Fluid Phase Equilib.* **2007**, *259*, 210–217.
(18) Shiflett, M. B.; Yokozeki, A. Liquid-Liquid Equilbria of Hydrofluoroethers and Ionic Liquid 1-Ethyl-3-methylimidazolium Bis(trifluoromethylsulfonyl)imide. *J. Chem. Eng. Data* **2007**, *52*, 2413–2418.
(19) Shiflett, M. B.; Yokozeki, A. Binary Vapor-Liquid and Vapor-Liquid-Liquid Equilibria of Hydrofluorocarbons (HFC-125 and HFC-143a) and Hydrofluoroethers (HFE-125 and HFE-143a) with Ionic Liquid [emim][Tf$_2$N]. *J. Chem. Eng. Data* **2008**, *53*, 492–497.
(20) Shiflett, M. B.; Yokozeki, A. Solubilities and Diffusivities of Carbon Dioxide in Ionic Liquids: [bmim][PF$_6$] and [bmim][BF$_4$]. *Ind. Eng. Chem. Res.* **2005**, *44*, 4453–4464.
(21) Shiflett, M. B.; Yokozeki, A. Solubility of CO$_2$ in Room-Temperature Ionic Liquid [hmim][Tf$_2$N]. *J. Phys. Chem. B* **2007**, *111*, 2070–2074.
(22) Yokozeki, A.; Shiflett, M. B. Hydrogen Purification using Room-Temperature Ionic Liquids. *Appl.Energy* **2007**, *84*, 351–361.
(23) Shiflett, M. B.; Kasprzak, D. J.; Junk, C. P.; Yokozeki, A. Phase Behavior of Carbon Dioxide + [bmim][Ac] Mixtures. *J. Chem. Thermodyn.* **2008**, *40*, 25–31.
(24) Yokozeki, A.; Shiflett, M. B.; Junk, C. P.; Grieco, L. M.; Foo, T. Physical and Chemical Absorptions of Carbon Dioxide in Room-Temperature Ionic Liquids. *J. Phys. Chem. B* **2008**, *112*, 16654–16663.
(25) Shiflett, M. B.; Yokozeki, A. Phase behavior of carbon dioxide in ionic liquids: [emim][acetate], [emim][trifluoroacetate], and [emim][acetate] + [emim][trifluoroacetate] mixtures. *J. Chem. Eng. Data* **2009**, *54*, 108–114.
(26) Meindersma, G. W.; Podt, A. J. G.; de Haan, A. B. Ternary liquid-liquid equilibria for mixtures of toluene + n-heptane + an ionic liquid. *Fluid Phase Equilib.* **2006**, *247*, 158–168.
(27) Meindersma, G. W.; Podt, A. J. G.; de Haan, A. B. Ternary Liquid-Liquid Equilibria for Mixtures of an Aromatic + an Aliphatic Hydrocarbon + 4-Methyl-N-butylpyridinium Tetrafluoroborate. *J. Chem. Eng. Data* **2006**, *51*, 1814–1819.
(28) Arce, A.; Earle, M. J.; Rodriguez, H.; Seddon, K. R. Separation of aromatic hydrocarbons from alkanes using the ionic liquid 1-ethyl-3-methylimidazolium bis{(trifluoromethyl) sulfonyl}amide. *Green Chem.* **2007**, *9*, 70–74.
(29) Łachwa, J.; Bento, I.; Teresa Duarte, M.; Canongia Lopes, J. N.; Rebelo, L. P. N. Condensed phase behavior of ionic liquid-benzene mixtures: congruent melting of a [emim][NTf$_2$]·C$_6$H$_6$ inclusion crystal. *Chem. Commun.* **2006**, 2445–2447.
(30) Blesic, M.; Canongia Lopes, J. N.; Rebelo, L. P. N. *Phase Equilibria in Ionic Liquid - Aromatic Compound Mixtures*; ACS Poster 128, ACS Meeting, Philadelphia, PA, August 19, 2008.
(31) Domańska, U.; Paduszyński, K. Phase Equilibria Study in Binary Systems (Tetra-*n*-butylphosphonium Tosylate Ionic Liquid + 1-Alcohol, or Benzene, or n-Alkylbenzene). *J. Phys. Chem. B* **2008**, *112*, 11054–11059.
(32) Domańska, U.; Casás, L. M. Solubility of Phosphonium Ionic Liquid in Alcohols, Benzene, and Alkylbenzenes. *J. Phys. Chem. B* **2007**, *111*, 4109–4115.
(33) Domańska, U.; Paduszyński, K. (Solid + liquid) and (liquid + liquid) phase equilibria measurements and correlation of the binary systems {tri-*iso*-butyl(methyl)phosphonium tosylate + alcohol, or +hydrocarbon}. *Fluid Phase Equilib.* **2009**, *278*, 90–96.
(34) Dittmar, H.; Butka, A.; Vale, R. V.; Schröer, W. Liquid-liquid phase transition in the ionic solutions of tetra-n-butylammonium chloride in o-xylene and ethylbenzene: Phase diagrams and corresponding state analysis. *J. Mol. Liq.* **2009**, *145*, 116–128.
(35) Lemmon, E. W.; McLinden, M. O.; Huber, M. L. *NIST reference fluid thermodynamic and transport properties - REFPROP*, (v. 7.0); National Institute of Standards and Technology: Gaithersburg, MD, 2002.
(36) Reid, R. C.; Prausnitz, J. M.; Poling, B. E. *The Properties of Gases & Liquids*, 4th ed.;McGraw-Hill: New York, 1987.
(37) Krummen, M.; Wasserscheid, P.; Gmehling, J. Measurement of Activity Coefficients at Infinite Dilution in Ionic Liquids Using the Dilutor Technique. *J. Chem. Eng. Data* **2002**, *47*, 1411.
(38) van Ness, C. H.; Abbott, M. M. *Classical Thermodynamics of Nonelectrolyte Solutions*; McGraw-Hill: New York, 1982.
(39) Hansen, C. M. *Hansen Solubility Parameter - A User's Handbook*, 1st ed.; CRC Press: Boca Raton, FL, 2000.
(40) Aki, S. N. V. K.; Brennecke, J. F.; Samanta, A. How polar are room-temperature ionic liquids. *Chem. Commun.* **2001**, 413–414.
(41) Fletcher, K. A.; Storey, I. A.; Hendricks, A. E.; Padney, S.; Padney, S. Behavior of the solvatochromic probes Reichardt's dye, pyrene, dansylamide, Nile Red and 1-pyrenecarbaldehyde within the room-temperature ionic liquid bmimPF$_6$. *Green Chem.* **2001**, *3*, 210–215.
(42) Dzyuba, S. V.; Bartsch, R. A. Expanding the polarity range of ionic liquids. *Tetrahedron Lett.* **2002**, *43*, 4657–4659.
(43) Reichardt, C. Polarity of ionic liquids determined empirically by means of solvatochromic pyridinium *N*-phenolate betaine dyes. *Green Chem.* **2005**, *7*, 339–351.
(44) Wakai, C.; Oleinikova, A.; Ott, M.; Weingärtner, H. How Polar Are Ionic Liquids? Determination of the Static Dielectric Constant of an Imidazolium-based Ionic Liquid by Microwave Dielectric Spectroscopy. *J. Phys. Chem. B* **2005**, *109*, 17028–17030.
(45) Jin, H.; O'Hare, B.; Dong, J.; Arzhantsev, S.; Baker, G. A.; Wishart, J. F.; Benesi, A. J.; Maroncelli, M. Physical Properties of Ionic Liquids Consisting of the 1-Butyl-3-Methylimidazolium Cation with Various Anions and the Bis(trifluoromethylsulfonyl)imide Anion with Various Cations. *J. Phys. Chem. B* **2008**, *112*, 81–92.
(46) Altshuller, A. P. The Dielectric Constants, Polarizations and Dipole Moments of some Alkylbenzenes. *J. Phys. Chem.* **1954**, *58*, 392–395.
(47) Huang, X.; Margulis, C.; Li, Y.; Berne, B. J. Why is the partial molar volume of CO$_2$ so small when dissolved in a room-temperature ionic liquid? Structure and dynamics of CO$_2$ dissolved in [bmim$^+$][PF$_6^-$]. *J. Am. Chem. Soc.* **2005**, *127*, 17842–17851.
(48) Choudhary, V. R.; Nayak, V. S.; Choudhary, T. V. Single-Component Sorption/Diffusion of Cyclic Compounds from Their Bulk Liquid Phase in H-ZSM-5 Zeolite. *Ind. Eng. Chem. Res.* **1997**, *36*, 1812–1818.
(49) Bikkulov, A. Z. Effect of the structure of the molecule on the properties of a selective solvent. *Khim. Tekhnol. Topliv Masel* **1996**, *2*, 10–13.
(50) Wasserscheid, P.; Welton, T., Eds. *Ionic Liquids in Synthesis*, 2nd ed.; Wiley-VCH: Weinheim, Germany, 2008.
(51) Hanke, C. G.; Johansson, A.; Harper, J. B.; Lynden-Bell, R. M. Why are aromatic compounds more soluble than aliphatic compounds in dimethylimidazolium ionic liquids? A simulation study. *Chem. Phys. Lett.* **2003**, *374*, 85–90.
(52) Harper, J. B.; Lynden-Bell, R. M. Macroscopic and microscopic properties of solutions of aromatic compounds in an ionic liquid. *Mol. Phys.* **2004**, *102*, 85–94.

(53) Shim, Y.; Choi, M. Y.; Kim, H. J. A. Molecular dynamics computer simulation study of room-temperature ionic liquids. I. Equilibrium solvation structure and free energetics. *J. Chem. Phys.* **2005**, *122*, 044510−1044510−12.

(54) Quiñonero, D.; Garau, C.; Frontera, A.; Ballester, P.; Costa, A.; Deyà, P. M. Structure and Binding Energy of Anion - π and Cation - π Complexes: A Comparison of MP2, RI-MP2, DFT, and DF-DFT Methods. *J. Phys. Chem. A* **2005**, *109*, 4632–4637.

(55) Dougherty, D. A. Cation - π Interactions in Chemistry and Biology: A New View of Benzene, Phe, Tyr, and Trp. *Science* **1996**, *271*, 163–168.

(56) Rowlinson, J. S.; Swinton, F. L. *Liquids and Liquid Mixtures*, 3rd ed.; Butterworth: London, 1982.

(57) Hildebrand, J.; Scott, R. L. *Regular Solutions*; Prentice-Hall, Inc.: Englewood Cliffs, NJ, 1962.

Received for review April 17, 2009. Accepted June 7, 2009. The present work was supported by DuPont Central Research and Development.

JE9003614